

# Negative Refraction Requires Strong Inhomogeneity

Igor Tsukerman\*

*Department of Electrical and Computer Engineering, The University of Akron, OH 44325-3904*

The paper establishes explicit lower bounds for the lattice cell size of periodic structures (metamaterials and photonic crystals) capable of supporting backward waves and producing negative refraction. At optical frequencies, this result implies strong inhomogeneity, in the sense that the cell size cannot be negligible relative to the vacuum wavelength and the Bloch wavelength.

PACS numbers: 41.20.-q, 41.20.Cv, 41.20.Jb, 42.25.Bs, 42.70.Qs

Negative refraction (electromagnetic waves bending the ‘wrong’ way at material interfaces) and the closely related phenomenon of backward waves (phase velocity at an obtuse angle with group velocity) have become one of the most intriguing areas of research in nanophotonics this century, with a number of books and review papers readily available, e.g. [1, 13, 26, 29, 30, 31], and hundreds of research papers published. As early as in the 1940s, Mandelshtam pointed out [25] that waves would refract negatively at the interface boundary between a regular and a backward-wave medium. In 1967, Veselago showed that media with simultaneously negative (relative) dielectric permittivity  $\epsilon_r$  and magnetic permeability  $\mu_r$  would support backward waves and exhibit other unusual behavior of wave propagation and refraction [35].

In 1999–2000, Pendry *et al.* [11] proved theoretically and Smith *et al.* [7] demonstrated experimentally negative refraction in an artificial medium with split-ring resonators. Furthermore, Pendry discovered that Veselago’s unusual ‘lens’ – a slab of a negatively refracting material – could produce a perfect image of a point source, thereby beating the diffraction limit [28].

Truly homogeneous materials, in the Veselago sense, are not currently known. Consequently, much effort has been devoted to the development of artificial metamaterials capable of supporting backward waves and producing negative refraction [2, 5, 7, 9, 10, 18, 20, 31, 33]. Separately from the progress in metamaterials, negative refraction has been observed and analyzed in singly and doubly periodic waveguides [38] and in photonic crystals [4, 8, 12, 14, 15, 16, 17, 22, 23, 27, 36].

All these intriguing findings have led to the presumption that there are two species of negative refraction, one occurring in photonic crystals and another one in metamaterials. Conceptually, the latter are viewed as prototypical ‘Veselago media’.

There are, indeed, salient differences between metamaterials and crystals in terms of the underlying structure, composition and fabrication (e.g. lossless dielectric inclusions vs. lossy metallic resonators of various kinds). On a more fundamental level, however, all such structures can be characterized by a periodically varying complex dielectric function, and from that point of view it is legitimate to examine possible *principal* differences between

metamaterials and photonic crystals. Importantly, can metamaterials, as a matter of principle, be (arbitrarily) close to an ideal homogeneous Veselago medium?

In the experimental and computational examples of the references cited above, the cell size as a fraction of the vacuum wavelength varies between  $\sim 0.11 \div 0.42$ . One would hope that further improvements in nanofabrication and design could bring the cell size down to a smaller fraction of the wavelength, thereby approaching the Veselago case of a homogeneous material. However, the main conclusion of the present paper is that the cell size is constrained not only by the fabrication technologies but by fundamental lower bounds as well.

The analysis in this paper relies on the usual 2D and 3D renditions of time-harmonic Maxwell’s equations, and it is assumed that bulk material parameters are applicable with a reasonable level of accuracy. At optical frequencies, the relative intrinsic permeability of all media can be set to unity ([24], §60; [39].) To streamline the mathematical development, we focus on square / cubic Bravais lattice cells with size  $a$  in 2D/3D and introduce dimensionless coordinates  $\tilde{x} = x/a$ , etc., so that in these tilde-coordinates the 2D / 3D problem is set up in the unit square / cube. The  $s$ -mode in the tilde-coordinates is described by the 2D wave equation

$$\tilde{\nabla}^2 E + \tilde{\omega}^2 \epsilon_r E = 0, \quad (1)$$

where  $E$  is a one-component electric field phasor and

$$\tilde{\omega} = \frac{\omega a}{c} = 2\pi \frac{a}{\lambda_0} \quad (2)$$

Here  $c$  and  $\lambda_0$  are the speed of light and the wavelength in free space, respectively. The relative permittivity  $\epsilon_r$  is a periodic function of coordinates over the lattice. In 3D, the governing equation is

$$\tilde{\nabla} \times \tilde{\nabla} \times \mathbf{E} = \tilde{\omega}^2 \epsilon \mathbf{E} \quad (3)$$

The fundamental solutions of the field equation in periodic structures are known to be Bloch-Floquet waves with a (yet undetermined) Bloch vector  $\mathbf{K}_B$ :

$$\mathbf{E}(\tilde{\mathbf{r}}) = \mathbf{E}_{\text{PER}}(\tilde{\mathbf{r}}) \exp(i\tilde{\mathbf{K}}_B \cdot \tilde{\mathbf{r}}) \quad (4)$$

where  $\tilde{\mathbf{r}}$  is the position vector. Subscript ‘PER’ implies periodicity with respect to any lattice vector

$(n_x a, n_y a, n_z a)$  with integer  $n_x, n_y, n_z$  in the 3D case.  $\mathbf{E}_{\text{PER}}$  can be expanded into a Fourier series

$$\mathbf{E}_{\text{PER}}(\tilde{\mathbf{r}}) = \sum_{\mathbf{n}} \tilde{\mathbf{e}}_{\mathbf{n}} \exp(i2\pi\mathbf{n} \cdot \tilde{\mathbf{r}}), \quad (5)$$

where  $\tilde{\mathbf{e}}_{\mathbf{n}}$  are the Fourier coefficients and index  $\mathbf{n}$  runs over the integer lattice  $\mathbb{Z}^2$  or  $\mathbb{Z}^3$  in 2D/3D.

For analysis and physical interpretation of energy flow, phase velocity and other properties of the Bloch wave, it is convenient to view it as a suite of spatial Fourier harmonics (plane waves) [3]. From (4) and (5),

$$\mathbf{E}(\tilde{\mathbf{r}}) = \sum_{\mathbf{n}} \mathbf{E}_{\mathbf{n}} \equiv \sum_{\mathbf{n}} \tilde{\mathbf{e}}_{\mathbf{n}} \exp(i2\pi\mathbf{n} \cdot \tilde{\mathbf{r}}) \exp(i\tilde{\mathbf{K}}_B \cdot \tilde{\mathbf{r}}) \quad (6)$$

The decomposition of the magnetic field is similar.

It is important to note from the outset [3] that the individual plane-wave components  $\mathbf{E}_{\mathbf{n}}$  of the electromagnetic Bloch wave do not satisfy Maxwell's equations in the periodic medium and therefore do not represent physical fields. Only taken together do these Fourier harmonics form a valid electromagnetic field.

It is straightforward to verify that the plane waves in the decomposition are orthogonal functions over the lattice cell (in the sense of standard vector  $\mathbf{L}_2$  inner product). Hence, by Parseval's theorem, the time- and cell-averaged Poynting vector  $\langle \mathbf{P} \rangle = \frac{1}{2} \langle \text{Re}\{\mathbf{E} \times \mathbf{H}^*\} \rangle$  can be represented as the sum of the Poynting vectors for the individual plane waves [3]:

$$\langle \mathbf{P} \rangle = \sum_{\mathbf{n}} \mathbf{P}_{\mathbf{n}}; \quad \mathbf{P}_{\mathbf{n}} = \frac{\pi n}{\tilde{\omega} \mu_0} |\tilde{\mathbf{e}}_{\mathbf{n}}|^2 \quad (7)$$

Group velocity  $\partial\tilde{\omega}/\partial\tilde{\mathbf{k}}$  is clearly the same for all plane wave components, and hence group velocity for the whole Bloch wave can be defined as  $v_g = \partial\tilde{\omega}/\partial\tilde{\mathbf{K}}_B$ . In cases of weak dispersion, this velocity indeed approximately represents signal velocity in the periodic medium [34, 37].

It is well known that in Fourier space the scalar wave equation (1) becomes

$$|\mathbf{K}_B + 2\pi\mathbf{n}|^2 \tilde{\mathbf{e}}_{\mathbf{n}} = \tilde{\omega}^2 \sum_{\mathbf{m}} \tilde{\mathbf{e}}_{\mathbf{n}-\mathbf{m}} \tilde{\mathbf{e}}_{\mathbf{m}} \quad (8)$$

where  $\tilde{\mathbf{e}}_{\mathbf{n}}$  are the Fourier coefficients of the dielectric permittivity  $\epsilon$ :

$$\epsilon = \sum_{\mathbf{n}} \tilde{\epsilon}_{\mathbf{n}} \exp(i2\pi\mathbf{n} \cdot \tilde{\mathbf{r}}) \quad (9)$$

Indeed, the right hand side of (8) is Fourier-space convolution corresponding to real-space multiplication  $\epsilon\mathbf{E}$ . The left hand side represents  $-\nabla^2$ .

Refraction at the interface between the periodic structure and air (or another homogeneous dielectric) depends not only on the *intrinsic* characteristics of the Bloch wave in the bulk, but also on the *extrinsic* conditions at the interface boundary – namely, the ‘excitation channel’ [3], i.e. the Fourier component of the Bloch wave that couples to the incident wave in the air [3, 13, 15]. Intrinsic

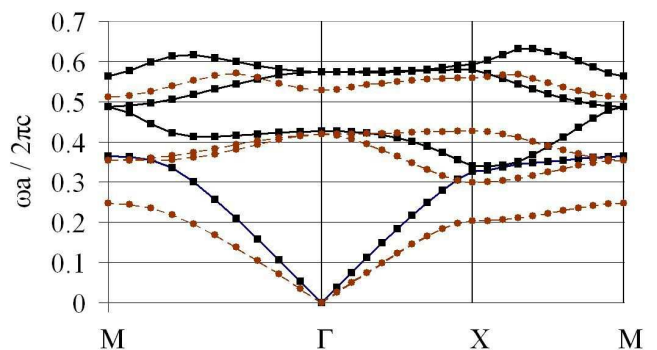


FIG. 1: The photonic band diagram of the Gajic *et al* crystal. TE modes ( $p$ -polarization, one-component  $H$  field) – squares, solid lines. TM modes ( $s$ -polarization, one-component  $E$  field) – circles, dashed lines.

properties include the forward or backward character of the wave – that is, whether the Poynting vector and phase velocity (if the latter can be properly defined) are at an acute or obtuse angle.

For illustration and further analysis, it is convenient to have a specific example in mind (however, the analysis and conclusions will be general). Consider the structure proposed by R. Gajic, R. Meisels *et al* [15, 16]. Their photonic crystal is a 2D square lattice of alumina rods in air. The radius of the rod is  $r_{\text{rod}} = 0.61$  mm, the lattice constant  $a = 1.86$  mm, so that  $r_{\text{rod}}/a \approx 0.33$ . The band diagram, computed using the plane wave method with 441 waves for  $s$ - and  $p$ -modes appears in Fig. 1 and, apart from the scaling factors, is very close to the one in [15, 16], where various cases of wave propagation and refraction are studied. In the context of this paper, of most interest is negative refraction for small Bloch numbers in the second band of the  $p$ -mode.

We observe that the TE2 dispersion curve is mildly convex around the  $\Gamma$  point ( $K_B = 0$ ,  $\omega a/2\pi c \approx 0.427$ ), indicating a negative group velocity for small positive  $K_B$  and a possible backward wave.

An additional condition for a backward wave must also be satisfied: the plane-wave component corresponding to the small positive Bloch number must be appreciable (or better yet, dominant). The distribution of Poynting components of the same wave is shown in Fig. 2. It is clear from the figure that the negative components outweigh the positive ones, so power flows in the negative direction. (Details can be found in [34].)

However, the normalized band diagram indicates that *negative refraction disappears in the homogenization limit* when the size of the lattice cells tends to zero, provided that other physical parameters, including frequency, are fixed. Indeed, the homogenization limit is obtained by considering the small cell size – long wavelength limit  $a \rightarrow 0$ ,  $\tilde{K} \rightarrow 0$  (see [6, 32] for additional mathemati-

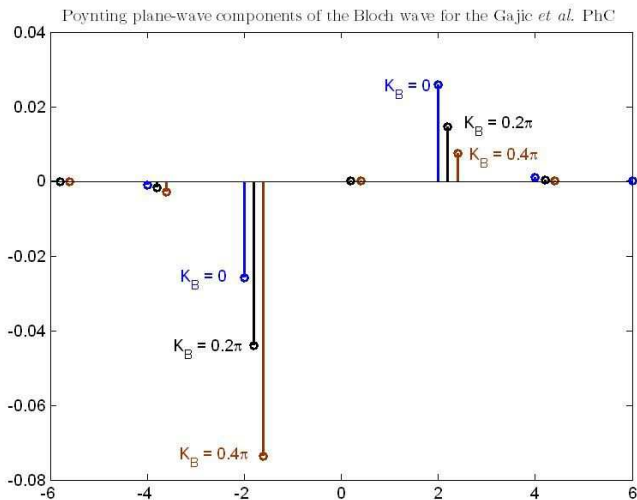


FIG. 2: The plane-wave Poynting components  $P_m$  for the Gajic *et al* crystal (arb. units). Second  $H$ -mode (TE2) near the  $\Gamma$  point on the  $\Gamma \rightarrow X$  line.

cal details on Floquet-based homogenization theory for Maxwell's equations). As these limits are taken, the problem and the dispersion curves *in the normalized coordinates* remain unchanged, but the operating point  $(\tilde{\omega}, \tilde{\mathbf{K}})$  approaches the origin along a fixed dispersion curve – the acoustic branch. In this case phase velocity in any given direction  $\hat{l}$ ,  $\omega/K_l = \tilde{\omega}/\tilde{K}_l$ , is well defined and equal to group velocity  $\partial\omega/\partial K_l$  simply by definition of the derivative. No backward waves can be supported in this regime.

This conclusion is not surprising from the physical perspective. As the size of the lattice cell diminishes, the operating frequency *increases*, so that it is not the absolute frequency  $\omega$  but the normalized quantity  $\tilde{\omega}$  that remains (approximately) constant. Indeed, a principal component of metamaterials with negative refraction is a resonating element [7, 30, 31, 33] whose resonance frequency is approximately inverse proportional to size [19].

It is pivotal in this paper to make a distinction between *strongly* and *weakly* inhomogeneous cases of wave propagation. The latter is intended to resemble an ideal ‘Veselago medium,’ with the Bloch wave being as close as possible to a long-length plane wave. Toward this end, the following conditions characterizing the weakly inhomogeneous backward-wave regime are put forth:

- The first-Brillouin-zone component of the Bloch wave must be dominant; this component then defines the phase velocity of the Bloch wave.
- The other plane-wave components collectively produce energy flow at an obtuse angle to phase velocity.

- The lattice cell size  $a$  is small relative to the vacuum wavelength  $\lambda_0$ ;  $a/\lambda_0 \ll 1$ .
- At the air-material interface, it is the long-wavelength, first-Brillouin-zone, plane wave component that serves as the excitation channel for the Bloch wave.

If any of the above conditions are violated, the regime will be characterized as *strongly inhomogeneous*: the EM wave can “see” the inhomogeneities of the material. By this definition, in the weakly inhomogeneous case the normalized Bloch wavenumber  $\tilde{K}_B$  must be small,  $\tilde{K}_B \equiv K_B a \ll \pi$ . Larger values of  $K_B$  would indicate a strongly inhomogeneous (or, synonymously, ‘photonic crystal’ or ‘grating’) regime, where the lattice size is comparable with the Bloch wavelength. As we shall see, under reasonable physical assumptions, backward waves cannot be supported in the weakly inhomogeneous case; strong inhomogeneity is required.

As a preliminary step in the analysis, it is instructive to examine the direction of power flow for small  $\tilde{K}_B$  in the lossless case (real  $\epsilon$ ). The average Poynting vector is, according to (7) and with a convenient normalization,

$$\tilde{P} \equiv 2\tilde{\omega}\mu_0 \langle P \rangle = K_B \left| \tilde{e}_0(\tilde{K}_B) \right|^2 +$$

$$\sum_{m=1}^{\infty} (\tilde{K}_B + 2\pi m) \left| \tilde{e}_m(\tilde{K}_B) \right|^2 + (\tilde{K}_B - 2\pi m) \left| \tilde{e}_{-m}(\tilde{K}_B) \right|^2 \quad (10)$$

The scalar form is used for notational convenience only; the vectorial case is quite similar. It is, however, essential to indicate explicitly that the Fourier amplitudes  $\tilde{e}_m$  depend on the Bloch parameter  $\tilde{K}_B$ . Since the waves corresponding to  $\pm\tilde{K}_B$  are complex conjugates of one another, we have  $\tilde{e}_{-m}(\tilde{K}_B) = \tilde{e}_m^*(-\tilde{K}_B)$ , and the expression for the Poynting vector becomes

$$\tilde{P} = \tilde{K}_B \left[ \left| \tilde{e}_0(\tilde{K}_B) \right|^2 + \sum_{m=1}^{\infty} \left( \left| \tilde{e}_m(\tilde{K}_B) \right|^2 + \left| \tilde{e}_m(-\tilde{K}_B) \right|^2 \right) \right] + 2\pi \sum_{m=1}^{\infty} m \left( \left| \tilde{e}_m(\tilde{K}_B) \right|^2 - \left| \tilde{e}_m(-\tilde{K}_B) \right|^2 \right) \quad (11)$$

The first two terms in (11) are directly proportional to  $\tilde{K}_B$ . To make this small parameter explicit in the third sum as well, we write

$$\tilde{P} = \tilde{K}_B \left[ \left| \tilde{e}_0 \right|^2 + \sum_{m=1}^{\infty} \left( \left| \tilde{e}_m(\tilde{K}_B) \right|^2 + \left| \tilde{e}_m(-\tilde{K}_B) \right|^2 \right) + 2\pi \sum_{m=1}^{\infty} m \frac{\partial \left| \tilde{e}_m \right|^2}{\partial \tilde{K}_B} \right] \quad (12)$$

For small  $\tilde{\omega}$ , the positive term  $\left| \tilde{e}_0 \right|^2$  in the square brackets tends to be dominant, making it difficult to produce a

negative power flow and a backward wave. This is so because the magnitudes of all spatial harmonics *except* for  $\tilde{e}_0$  are for small  $\tilde{\omega}$  constrained by (8):

$$|\tilde{e}_n| \leq \tilde{\omega}^2 \left| \tilde{\mathbf{K}}_B + 2\pi\mathbf{n} \right|^{-2} \|\tilde{\epsilon}\|_{l_2}, \quad \|\tilde{\epsilon}\|_{l_2} = 1, \quad n \neq 0 \quad (13)$$

The arguments above suggest that there must be a lower bound for the relative cell size  $a/\lambda_0 = \tilde{\omega}/2\pi$  when the medium could still support backward waves. To the best of my knowledge, this question has not so far been posed explicitly in the literature.

In the remainder, we investigate the constraints on the periodic *in the weakly inhomogeneous backward-wave regime*. This implies that  $\tilde{K}_B = K_B a \ll 1$ . To simplify mathematical analysis, we focus on the limiting case  $K_B = 0$ , but the conclusions will apply, by physical continuity, to small  $\tilde{K}_B$ . We first turn to the *s*-mode governed by the 2D equation (1). For  $\tilde{\omega} \neq 0$  and  $\eta = \tilde{\omega}^{-2}$ ,

$$\epsilon E = -\eta \tilde{\nabla}^2 E \quad (14)$$

Further analysis relies on the inversion of  $\tilde{\nabla}^2$ . To do this unambiguously, let us split  $E$  up into the zero-mean term  $E_\perp$  and the remaining constant  $E_0$ :  $E = E_0 + E_\perp$ . Symbol ‘ $\perp$ ’ indicates orthogonality to the null space of the Laplacian (i.e. to constants). To eliminate the constant component  $E_0$ , we integrate (14) over the lattice cell. Integrating by parts and noting that the boundary term vanishes due to the periodic boundary conditions ( $K_B = 0$ ), we get

$$E_0 = -\tilde{\epsilon}_0^{-1} \int_{\Omega} \epsilon E_\perp d\Omega, \quad \tilde{\epsilon}_0 \neq 0$$

(The exceptional case  $\tilde{\epsilon}_0 = 0$  is mathematically quite intricate and may constitute a special topic for future research.) With  $E_0$  eliminated, the eigenvalue problem for  $E_\perp$  becomes

$$\epsilon \left[ E_\perp - \tilde{\epsilon}_0^{-1} \int_{\Omega} \epsilon E_\perp d\Omega \right] = -\eta \tilde{\nabla}^2 E_\perp$$

Since  $E_\perp$  by definition is zero-mean,

$$\tilde{\nabla}_\perp^{-2} \{ \epsilon [E_\perp - \tilde{\epsilon}_0^{-1} (\int_{\Omega} \epsilon E_\perp)] \} = -\eta E_\perp \quad (15)$$

where  $\tilde{\nabla}_\perp^{-2}$  is the zero-mean inverse of the Laplacian. Fourier analysis easily shows that this inverse is bounded (the Poincaré inequality):  $\|\tilde{\nabla}_\perp^{-2}\| \leq (4\pi^2)^{-1}$ . Then, taking the norm of both sides of (15), we get

$$|\eta| \leq (4\pi^2)^{-1} |\epsilon|_{\max} (1 + |\epsilon|_{\max}/|\tilde{\epsilon}_0|) \quad (16)$$

This result, that can be viewed as a generalization of the Poincaré inequality to cases with variable  $\epsilon_r$ , leads to a simple lower bound for the lattice cell size, with the mean and maximum values of  $\epsilon$  as parameters:

$$\left( \frac{a}{\lambda_0} \right)^2 = \frac{\tilde{\omega}^2}{4\pi^2} \geq \frac{1}{|\epsilon|_{\max} (1 + |\epsilon|_{\max}/|\tilde{\epsilon}_0|)} \quad (17)$$

Turning now to the vector field formulation (3), we deal with 2D and 3D cases simultaneously and rewrite the field equation as

$$\epsilon \mathbf{E} = -\eta \tilde{\nabla} \times \tilde{\nabla} \times \mathbf{E} \quad (18)$$

The  $\tilde{\nabla} \times \tilde{\nabla} \times$  operator can be inverted unambiguously if the result, denoted with  $(\tilde{\nabla} \times)_\perp^{-2}$ , is sought in the functional space  $\mathbf{H}_\perp^1(\Omega)$  of divergence-free zero-mean fields. For any such field  $\mathbf{u}$ ,  $\tilde{\nabla} \times \tilde{\nabla} \times \mathbf{u} = -\tilde{\nabla}^2 \mathbf{u}$  and hence

$$\left\| \tilde{\nabla}^2 \mathbf{u} \right\|_2^2 = (\tilde{\nabla} \times \tilde{\nabla} \times \mathbf{u}, \tilde{\nabla} \times \tilde{\nabla} \times \mathbf{u})$$

$$= (\tilde{\nabla}^2 \mathbf{u}, \tilde{\nabla}^2 \mathbf{u}) \geq (4\pi^2)^2 (\mathbf{u}, \mathbf{u}) = (4\pi^2)^2 \|\mathbf{u}\|_2^2$$

This implies that the inverse curl-curl, considered as an operator with its range in  $\mathbf{H}_\perp^1$ , is bounded:

$$\left\| (\tilde{\nabla} \times)_\perp^{-2} \right\| \leq (4\pi^2)^{-1} \quad (19)$$

The relevant splitting of  $\mathbf{E}$  is into the zero-mean divergence-free term  $\mathbf{E}_\perp \in \mathbf{H}_\perp^1$  and the curl-free remainder [40]  $\mathbf{E}_0 = -\nabla \phi_0$  (the Helmholtz decomposition):  $\mathbf{E} = \mathbf{E}_\perp - \tilde{\nabla} \phi_0$ . Field  $\mathbf{E}_\perp$  is in fact, up to the factor  $i\tilde{\omega}$ , the magnetic vector potential with the Coulomb (zero-divergence) gauge.

Taking divergence (in the distributional sense) of the governing equation (18) and integrating over the cell, one eliminates the electrostatic term  $\tilde{\nabla} \phi_0$  and arrives at an eigenvalue problem for  $\mathbf{E}_\perp$ :

$$\epsilon \left( \mathbf{E}_\perp - \nabla \mathcal{L}_\epsilon^{-1} \tilde{\nabla} \cdot (\epsilon \mathbf{E}_\perp) \right) = -\eta \tilde{\nabla} \times \tilde{\nabla} \times \mathbf{E}_\perp$$

assuming that the electrostatic operator  $\mathcal{L}_\epsilon = \tilde{\nabla} \cdot \epsilon \tilde{\nabla}$  is nonsingular. Equivalently, since  $\mathbf{E}_\perp$  is by definition divergence-free and zero-mean,

$$(\tilde{\nabla} \times)_\perp^{-2} \{ \epsilon [\mathbf{E}_\perp - \nabla \mathcal{L}_\epsilon^{-1} \tilde{\nabla} \cdot (\epsilon \mathbf{E}_\perp)] \} = -\eta \mathbf{E}_\perp \quad (20)$$

an upper bound for  $\eta$  can be obtained by taking the  $\mathbf{L}_2$ -norms of both sides, with (19) in mind:

$$|\eta| \leq (4\pi^2)^{-1} |\epsilon|_{\max} (1 + |\lambda|_{\max}(\mathcal{L}_\epsilon^{-1}) |\epsilon|_{\max}) \quad (21)$$

This estimate is analogous to the scalar one (16), except that the maximum eigenvalue  $|\lambda|_{\max}(\mathcal{L}_\epsilon^{-1})$  (not to be confused with the wavelength) appears instead of the inverse mean value  $|\tilde{\epsilon}_0|^{-1}$  of the permittivity. This eigenvalue is bounded unless the operating frequency is close to the quasi-static plasmon resonance value. In the most general situation, no simple estimate of  $|\lambda|_{\max}(\mathcal{L}_\epsilon^{-1})$  is available, but it can be computed numerically using a number of algorithms (see e.g. [34]) for any given distribution of  $\epsilon$  in the lattice cell.

At the same time, there are practically important situations where the bound for  $\eta$  can be made more explicit.

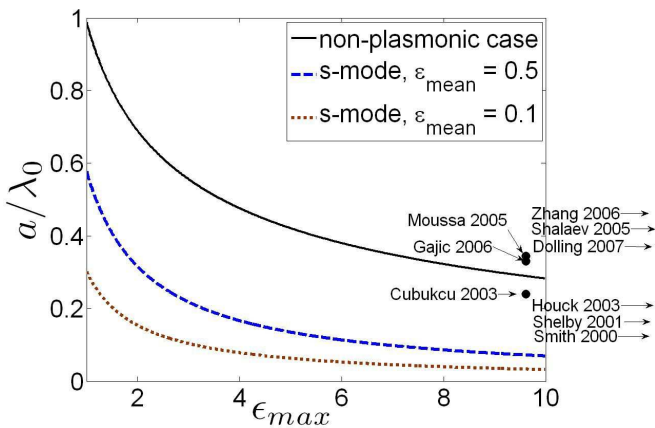


FIG. 3: Bounds on the normalized cell size and a few representative data points from the literature.

One such case is that of non-plasmonic materials, when  $\epsilon \geq \epsilon_{\min} > 0$  throughout the lattice cell. Then

$$|\lambda|_{\max}(\mathcal{L}_\epsilon^{-1}) \leq \epsilon_{\min}^{-1} |\lambda|_{\max}(\nabla_{\perp}^{-2}) \leq (4\pi^2 \epsilon_{\min})^{-1}$$

and from the estimate (21) for  $|\eta|$  the following bound on the normalized cell size emerges:

$$\left(\frac{a}{\lambda_0}\right)^2 = \left(\frac{\tilde{\omega}}{2\pi}\right)^2 = \frac{1}{4\pi^2 |\eta|} \geq \frac{1}{|\epsilon|_{\max} (1 + |\epsilon|_{\max}/(4\pi^2 \epsilon_{\min}))} \quad (22)$$

The lower bounds (17) and (22) are plotted as a function of  $|\epsilon|_{\max}$  in Fig. 3, for  $\epsilon_{\min} = 1$  and two values of  $\tilde{\epsilon}_0$  (0.5 and 0.1). For illustration, several representative data points (both theoretical and experimental) from the literature are also shown in the figure. In the microwave regime, when metals are very good conductors and consequently  $|\epsilon|_{\max}$  is high, the theoretical bound for the cell size is non-restrictive and the respective data points (Smith, Shelby, Houck, and others) easily turn up above the relevant theoretical curve; these points lie off the chart in Fig. 3.

The Cubukcu *et al* data point lies *below* the theoretical line (22); however, there is no contradiction because in this instance negative refraction occurs in the vicinity of the M point, where the Bloch wavelength and the lattice cell size are comparable. This constitutes, by our definition, a strongly inhomogeneous case to which the theoretical bound does not apply.

The Moussa and Gajic data points for non-metallic crystals lie only slightly above the theoretical bound, indicating that this bound can be approached in some cases. Still, it must be stressed that the theoretical limits on the cell size are *necessary*, but in general *not sufficient*, conditions for negative refraction. A sufficiently large lattice cell size makes it *possible* for higher-order Fourier harmonics of the Bloch wave to outweigh the

first-Brillouin-zone harmonic, but does not guarantee that they will do so and that they will have the desirable sign.

Another case where the theoretical bound (21) can be made more explicit is that of a lossless host medium,  $\epsilon = \epsilon_h$ , with embedded ‘inclusions’  $\epsilon = \epsilon_i = \epsilon'_i + i\epsilon''_i$  (spheres, split-ring resonators, fishnets, horseshoes, rods, etc.). The eigenvalue  $|\lambda|_{\max}(\mathcal{L}_\epsilon)^{-1} = |\lambda|_{\min}^{-1}(\mathcal{L}_\epsilon)$  can be estimated from the electrostatic energy functional

$$(\epsilon \nabla \phi, \nabla \phi) = \epsilon_h W_h + (\epsilon'_i + i\epsilon''_i) W_i$$

where  $W_{h,i} = \int_{\Omega_{h,i}} |\nabla \phi|^2 d\Omega$ . Then  $|(\epsilon \nabla \phi, \nabla \phi)|^2$  is a quadratic form with respect to  $W_{h,i}$  and can be bounded by direct evaluation of its minimum eigenvalue. The end result, for small losses  $\epsilon''_i \ll \epsilon_h + |\epsilon_i|$ , is

$$|\lambda|_{\min}^2(\mathcal{L}_\epsilon) \gtrsim \frac{\epsilon_h^2 \epsilon_i'^2}{2(\epsilon_h^2 + |\epsilon_i|^2)}$$

This estimate can be used in conjunction with the general bound (21).

In summary, it has been proved that periodic structures capable of supporting backward waves and producing negative refraction in the optical range must be strongly inhomogeneous. More precisely, the lattice cell size, as a fraction of the vacuum wavelength and/or the Bloch wavelength, must be above certain thresholds established in this paper. These thresholds contain the maximum, minimum and mean values of the complex dielectric permittivity as key parameters. In the presence of good conductors (e.g. at microwave frequencies) such theoretical constraints are not very restrictive. However, at optical frequencies and/or for non-metallic structures the bounds on the cell size must be honored and may help to design metamaterials and photonic crystals with desired optical properties.

---

\* Electronic address: igor@uakron.edu;  
URL: <http://coel.ecgf.uakron.edu/~igor/>

- [1] G.V. Eleftheriades and K.G. Balmain. Wiley-IEEE Press, 2005.
- [2] A.A. Houck *et al.* *Phys. Rev. Lett.*, 90(13):137401, 2003.
- [3] B. Lombardet *et al.* *J. Opt. Soc. Am. B*, 22:1179–1190, 2005.
- [4] C. Luo *et al.* *Phys. Rev. B*, 65(20):201104, 2002.
- [5] C.G. Parazzoli *et al.* *Phys. Rev. Lett.*, 90(10):107401, 2003.
- [6] D. Sjöberg *et al.* *Multiscale Mod & Sim*, 4(1):149–171, 2005.
- [7] D.R. Smith *et al.* *Phys. Rev. Lett.*, 84(18):4184–4187, 2000.
- [8] E. Cubukcu *et al.* *Phys. Rev. Lett.*, 91(20):207401, 2003.
- [9] G. Dolling *et al.* *Optics Lett*, 31(12):1800–1802, 2006.
- [10] G. Dolling *et al.* *Optics Lett*, 32(1):53–55, 2007.
- [11] J.B. Pendry *et al.* *IEEE Trans. on Microwave Theory and Techniques*, 47(11):2075–2084, 1999.

- [12] M.S. Wheeler *et al.* *Phys Rev B*, 73(4):045105, 2006.
- [13] P.A. Belov *et al.* *J. of Communications Technology and Electronics*, 49(11):1199–1207, 2004.
- [14] P.V. Parimi *et al.* *Phys Rev Letters*, 92(12):127401, 2004.
- [15] R. Gajic *et al.* *Opt. Express*, 13:8596–8605, 2005.
- [16] R. Meisels *et al.* *Opt. Express*, 14:6766–6777, 2006.
- [17] R. Moussa *et al.* *Phys Rev B*, 71(8):085106, 2005.
- [18] R.A. Shelby *et al.* *Science*, 292(5514):77–79, 2001.
- [19] S. Linden *et al.* *IEEE Journal of Selected Topics in Quantum Electronics*, 12(6):1097–1105, 2006.
- [20] S. Zhang *et al.* *J. Opt. Soc. Am. B*, 23(3):434–438, 2006.
- [21] W. Cai *et al.* *Opt. Express*, 15:3333–3341, 2007.
- [22] S. Foteinopoulou and C. M. Soukoulis. *Phys Rev B*, 72(16):165112, 2005.
- [23] S. Foteinopoulou and C.M. Soukoulis. *Phys. Rev. B*, 67(23):235107, 2003.
- [24] L.D. Landau and E.M. Lifshitz. *Electrodynamics of Continuous Media*. Oxford; New York: Pergamon, 1984.
- [25] L.I. Mandelshtam. *Polnoe Sobranie Trudov, v. 2,5*. Akademiia Nauk SSSR, 1947, 1950.
- [26] P.W. Milonni. *Fast Light, Slow Light and Left-Handed Light*. Taylor & Francis, 2004.
- [27] M. Notomi. *Phys. Rev. B*, 62(16):10696–10705, 2000.
- [28] J.B. Pendry. *Phys. Rev. Lett.*, 85(18):3966–3969, 2000.
- [29] J.B. Pendry and D.R. Smith. *Phys. Today*, 57:37–43, 2004.
- [30] S.A. Ramakrishna. *Rep. Prog. Phys.*, 68:449–521, 2005.
- [31] V.M. Shalaev. *Nature Photonics*, 1:41–48, 2006.
- [32] D. Sjöberg. *Multiscale Mod & Sim*, 4(3):760–789, 2005.
- [33] D. R. Smith and D. C. Vier. In *Proc SPIE, 5359*, pages 52–63, 2004.
- [34] I. Tsukerman. *Computational Methods for Nanoscale Applications: Particles, Plasmons and Waves*. Springer, 2007. (To be published.)
- [35] V.G. Veselago. *Sov Phys Uspekhi*, 10(4):509–514, 1968.
- [36] V. Yannopapas and A. Moroz. *J. Phys.: Condensed Matter*, 17(25):3717–3734, 2005.
- [37] P. Yeh. *J. Opt. Soc. Am.*, 69(5):742–756, 1979.
- [38] R. Zengerle. *J. Mod. Optics*, 34:1589–1617, 1987.
- [39] Artificial magnetism can be created in periodic dielectric structures at optical frequencies [19, 21]. The equivalent ‘mesoscopic’ permeability may then be different from  $\mu_0$ , but the intrinsic *microscopic* permeability of the materials involved is still  $\mu_0$ .
- [40] Curl-free fields are representable as gradients if the domain is simply connected; this is certainly true for any Bravais lattice cell.